

Supporting Information

Benitez-Alfonso *et al.* 10.1073/pnas.0808717106

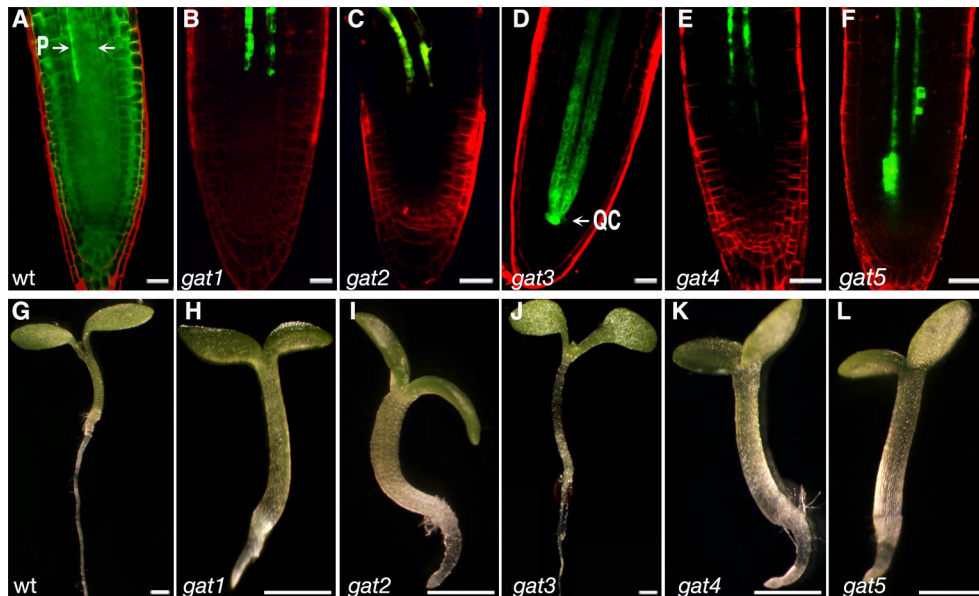


Fig. S1. GFP transport and seedling phenotypes of WT and *gat* mutants. (A) WT seedlings expressing *pSUC2-GFP* show GFP diffusion out of the phloem (P, arrows) into the root meristem. (B–F) The mutants *gat1*, 2, 4, and 5 show severe restriction in GFP transport out of the phloem, and in *gat3* (D) the transport is restricted to the stele and quiescent center (QC, arrow). Seedling phenotypes of (G) WT and (H–L) *gat* mutants at 6 dpv show that *gat1*, 2, 4, and 5 seedlings are smaller than WT seedlings. Scale bar represents 20 μm in A–F and 1 mm in G–L.

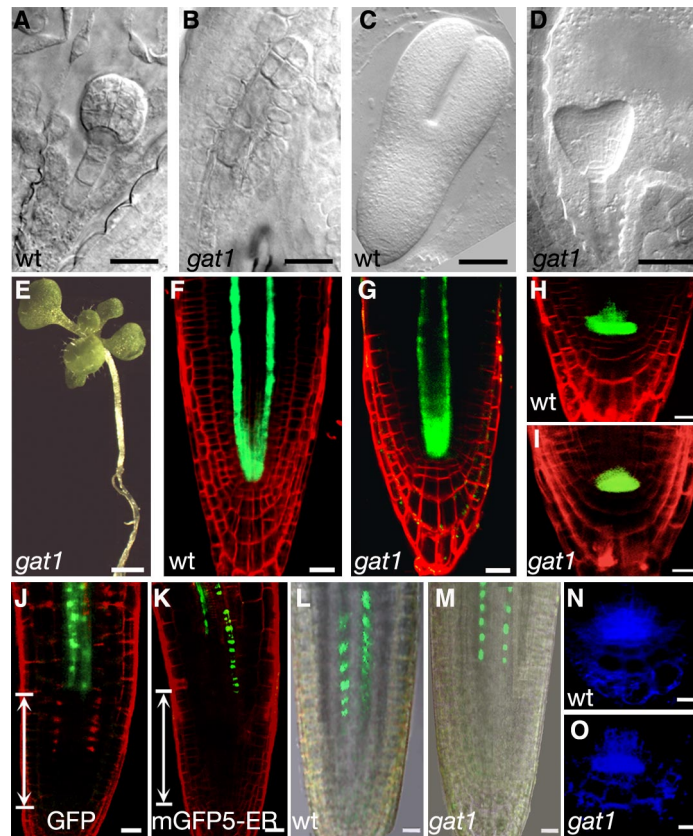


Fig. S2. *gat1* embryo and sucrose rescue phenotype, phloem, and QC identity. WT and *gat1* siblings at globular (A, B) and torpedo (C, D) stages show that *gat1* embryos develop more slowly, but they have normal morphology. (E) The partially rescued phenotype of *gat1* seedling grown in 1% sucrose medium. GFP reporters, specific for the pro-vasculature (JYB697 in F and G) and the QC (JYB1234 in H and I), show similar expression in WT and *gat1*. (J, K) Confocal images of *gat1* roots expressing p*SUC2-GFP* (GFP in J) and p*SUC2-mGFP5-ER* (mGFP5-ER in K). The distance from the QC to the lower limit of the GFP-expressing cells (white arrows) was similar in mutants expressing a non-mobile version of GFP (mGFP5-ER; $128 \pm 13 \mu\text{m}$) and mutants expressing cytoplasmic GFP (GFP; $124 \pm 17 \mu\text{m}$), indicating that cytoplasmic GFP is confined to the phloem CC in *gat1*. (L–O) Confocal images of *gat1* and WT roots expressing a GFP translational fusion of ALTERED PHLOEM DEVELOPMENT (p*APL-APL-GFP*) (L, M) and a transcriptional CFP reporter of *PLETHORA1* (p*PLT1-CFP*) (N, O). Mutant and WT roots showed normal expression of these reporters, suggesting that the phloem and QC identities are not affected in *gat1*. Scale bars represent $20 \mu\text{m}$ in A–D and F–O and 1 mm in E.

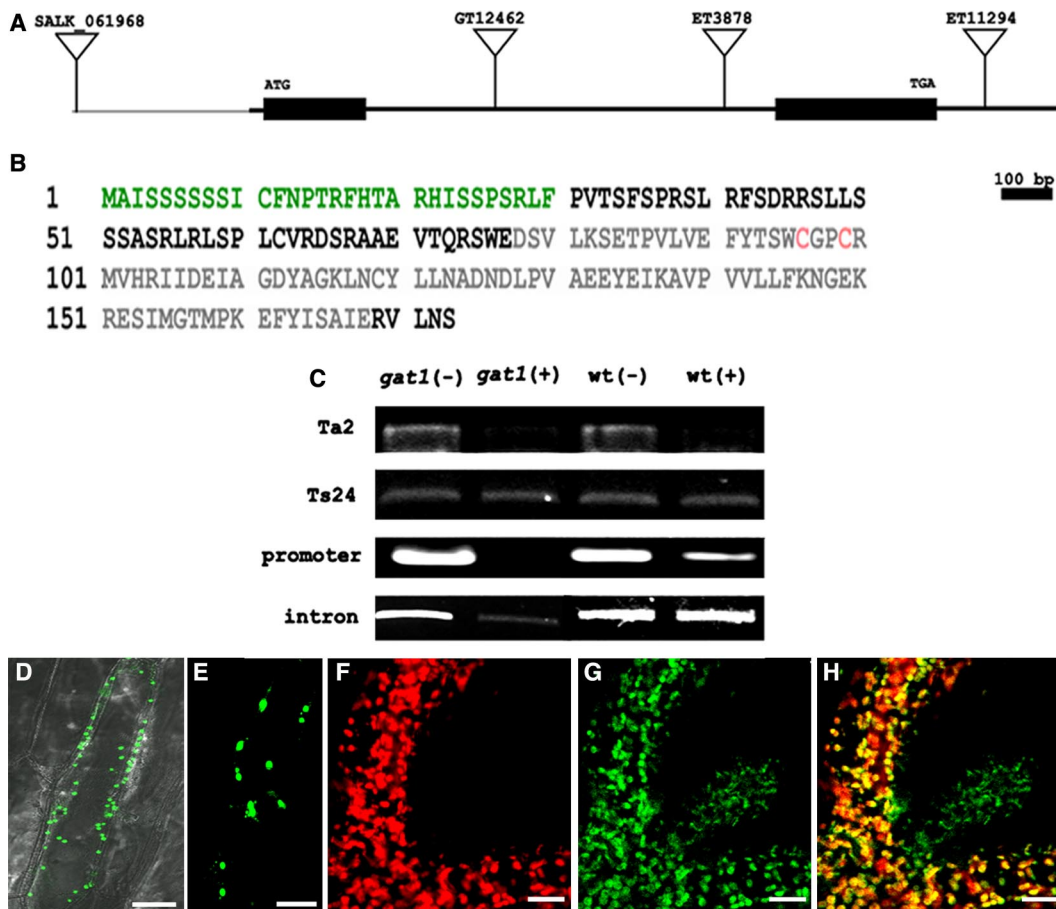


Fig. S3. *GAT1* alleles and intracellular localization. (A) The *GAT1* gene has 2 exons, indicated by black boxes. T-DNA and transposon insertions in the promoter and coding region were identified, and their positions are indicated. (B) The gene encodes a small protein with a thioredoxin domain (shown in gray), conserved cysteines (shown in red), and a plastidial targeting sequence (shown in green), as predicted by the program ChloroP 1.1 (1). Methylation assays were performed as described (2). In brief, 1 μ g genomic DNA from WT and mutant plants was digested with McrBC enzyme (New England Biolabs). Equal aliquots of digested (+) and non-digested (-) DNA were amplified with primers to a transposon (*TA2*) and to a non-methylated gene (*T24H24*) as positive and negative controls, respectively. (C) Primers that amplify *GAT1* promoter or the intron showed reduced PCR amplification using *gat1* genomic DNA digested with McrBC (*gat1(+)*) as template in comparison with WT (*wt(+)*) and with undigested DNA (*gat1(-)*, *wt(-)*), suggesting hypermethylation in *gat1-1*. To confirm these results, we crossed *gat1* to deficient in DNA methylation 1 (*ddm1*) (3). Analysis of *gat1-1/ddm1* double mutants showed that *ddm1* partially rescued the *gat1-1* trafficking phenotype (not shown). *GAT1*:YFP transient expression in (D) onion and in (E) *Arabidopsis* leaves shows localization in presumed plastids. (F–H) Confocal images of seedling shoots from plants overexpressing *GAT1*:YFP show green fluorescence in both photosynthetic and non-photosynthetic tissues that co-localizes with chlorophyll red autofluorescence. Scale bars represent 20 μ m.

Callose quantitation in the root tip

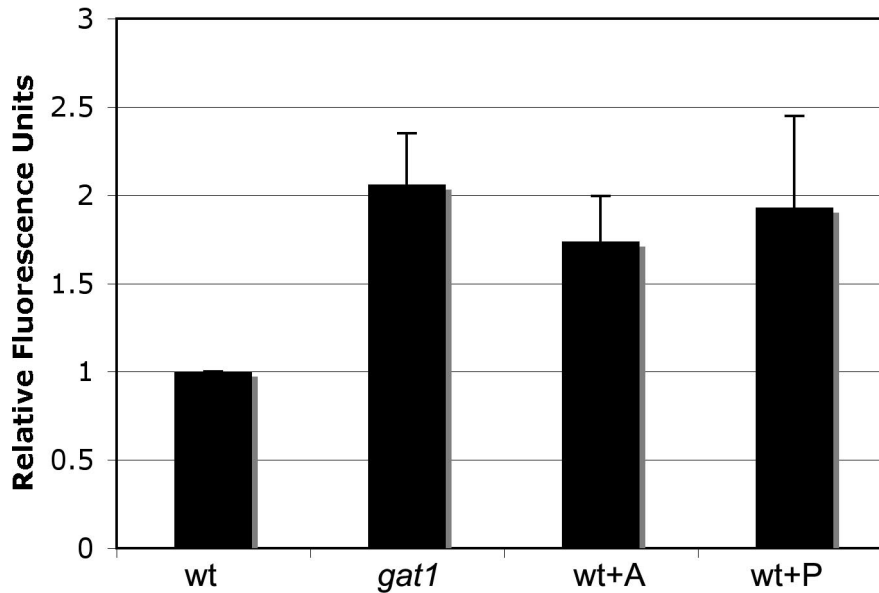


Fig. S4. Callose levels are higher in *gat1* mutants and in WT (wt) plants treated with oxidants. Callose levels in *gat1* or in seedlings treated with alloxan (wt+A) and paraquat (wt+P) were quantified by aniline blue staining of the root meristem. Four biological replicates were imaged in the fluorescence microscope under UV light. Analysis of the fluorescence intensity per μm of area was performed with the program ImageJ (<http://rsbweb.nih.gov/ij/>). The WT value was set arbitrarily at 1, and other values were calculated relative to the WT. The graph shows that *gat1* and oxidant-treated seedlings accumulated about twice the amount of callose found in WT ($P < 0.001$). Callose also was extracted from fresh tissues and quantified as described (4). Fluorescence was measured at 393-nm excitation and 479-nm emission in a Synergy 4 microplate reader (Biotek), using Pachyman (PE) as reference. Callose concentration (expressed in units of PE per gram of fresh weight) was detected in pools of 40 seedlings at 6 dpv and was found to be significantly higher in the mutants (62 ± 5) than in WT (46 ± 5). The values are means \pm SD of 4 independent replicas, and the results are statistically significant following the student's *t*-test ($P < 0.005$).

1. Emanuelsson O, Nielsen H, von Heijne G (1999) ChloroP, a neural network-based method for predicting chloroplast transit peptides and their cleavage sites. *Protein Sci* 8:978–984.
2. Rabinowicz PD, et al. (2003) Genes and transposons are differentially methylated in plants, but not in mammals. *Genome Research* 13:2658–2664.
3. Jeddeloh JA, Bender J, Richards EJ (1998) The DNA methylation locus DDM1 is required for maintenance of gene silencing in *Arabidopsis*. *Genes Dev* 12:1714–1725.
4. Sivaguru M, et al. (2000) Aluminum-induced 1 \rightarrow 3-beta-D-glucan inhibits cell-to-cell trafficking of molecules through plasmodesmata. A new mechanism of aluminum toxicity in plants. *Plant Physiol* 124:991–1006.

Table S1. Total chlorophylls and H₂O₂ content of *gat1* mutants and transgenic lines

Samples	WT Seedlings	<i>gat1</i> Seedlings	WT Leaves	<i>pSAG12:GAT1</i> Leaves	WT Leaves ^a	<i>pSAG12:GAT1</i> Leaves ^a
Total chlorophylls (mg/g fresh weight)	0.46 ± 0.02	0.19 ± 0.04	0.61 ± 0.1	0.74 ± 0.03	0.4 ± 0.02	0.68 ± 0.1
Soluble peroxides (nmol H ₂ O ₂ /g fresh weight)	29.4 ± 6	48.4 ± 7	75.6 ± 10	33.9 ± 7.7	119 ± 8.3	56.4 ± 2.0

^aDetached leaves induced to senescence by dark treatment for 5 days.

Plants were grown in long-day conditions in MS plates (seedlings) or soil (leaves). Leaf samples (third and fourth leaves of plants grown for 21 days) or pools of 30 seedlings at 6 dpv were harvested directly into liquid nitrogen. Total chlorophyll was extracted in 80% acetone and quantified by spectrophotometric analysis as previously described (1). The samples were measured using 1 ml of extracts in 1-cm cuvettes, and total chlorophyll, in mg/l, was calculated according to the formula $20.2A_{645} + 8.02A_{663}$ (1). To evaluate hydrogen peroxide concentration, plant tissues were extracted in trichloroacetic acid, and water-soluble peroxides were quantified by the eFOX method as previously described (2). A standard curve was constructed using different concentrations of hydrogen peroxide, and the results were expressed in nmol H₂O₂. Data are means ± SD per gram of fresh weight calculated in 3 independent replicas. The results show that *gat1* mutants have reduced levels of total chlorophyll pigments but higher amounts of soluble peroxides, suggesting that the oxidative state of the mutant induces chlorophyll breakdown. *pSAG12-GAT1* leaves were found to retain more chlorophyll pigments than WT after senescence induction, but no significant differences were found before the induction. H₂O₂ concentration also was evaluated in *pSAG12-GAT1* vs. WT leaves, and a significant decrease was detected in the transgenic plants, suggesting that the ectopic expression of GAT1 increased the reductive potential in the leaves, probably protecting against chlorophyll degradation. All differences described were statistically significant following the student's *t*-test ($P < 0.05$).

1. McCabe MS, et al. (2001) Effects of *P(SAG12)-IPT* gene expression on development and senescence in transgenic lettuce. *Plant Physiol* 127:505–516.
2. Cheeseman JM (2006) Hydrogen peroxide concentrations in leaves under natural conditions. *J Exp Bot* 57:2435–2444.

